Radiotherapy and Oncology 137 (2019) 77–82

Contents lists available at ScienceDirect

Radiotherapy and Oncology

journal homepage: www.thegreenjournal.com

Original Article

Comparison between bone matching and marker matching for evaluation of intra- and inter-fractional changes in accumulated dose of carbon ion radiotherapy for hepatocellular carcinoma

Yoshiki Kubota [a,*], Hiroyuki Katoh [b], Kei Shibuya [a], Shintaro Shiba [a], Satoshi Abe [c], Makoto Sakai [a], Daichi Yuasa [c], Kazuhisa Tsuda [c], Tatsuya Ohno [a], Takashi Nakano [a]

[a] Gunma University Heavy Ion Medical Center; [b] Kanagawa Cancer Center; and [c] Department of Radiology, Gunma University Hospital, Japan

ARTICLE INFO

Article history:
Received 27 November 2018
Received in revised form 8 March 2019
Accepted 18 April 2019
Available online 9 May 2019

Keywords:
Carbon ion radiotherapy
Accumulated dose distribution
Intra- and inter-fractional anatomical change
Tumor matching
Bone matching
Hepatocellular carcinoma

ABSTRACT

Background and purpose: To determine whether bone matching (BM) or marker matching (MM) is the better positioning technique for carbon ion radiotherapy (CIRT) of primary hepatocellular carcinoma (HCC), we prospectively evaluated accumulated dose distributions with respect to intra- and inter-fractional anatomical changes.

Materials and methods: The accumulated doses in ten patients with HCC were evaluated, with the doses being calculated with respect to inter-fractional changes (InterDose) on treatment-room CT images on day 1 or day 2 of therapy (RefCT). This was accomplished by warping 3-day CT dose distributions to the RefCT through deformable registration. The accumulated doses were also calculated with respect to intra-fractional change (IntraDose) calculated by warping dose distributions for three 4DCT phases to the RefCT. Each dose was evaluated using dose–volume parameters for the clinical target volume (CTV) percentages receiving greater than 95% of the prescription dose (V_{95}).

Results: The InterDose CTV V_{95} values (mean [range]) were BM: 98.74% (95.62–100%), MM: 99.79% (98.55–100%), and the IntraDose values were BM: 99.46% (98.10–100%), MM: 99.74% (98.91–100%). Although all cases were acceptable with either matching method, MM provided better values than BM.

Conclusion: MM is a better positioning technique than BM for ensuring the target dose during and between fractions of CIRT. However, further analysis is required as our study included only a low number of cases.

Particle beams, especially carbon ion beams, are characterized by Bragg peak and a steep lateral penumbra that minimize damage to surrounding normal tissues while effectively concentrating damage on the tumor [1–3]. However, because the sharper borders of the dose distribution are highly position-sensitive, the actual dose may differ from the prescribed dose if either the tumor position shifts or the water equivalent path length (WEL) to the tumor changes. Tumors of mobile organs such as the lung [4,5], liver [6], and pancreas may undergo greater changes [7], so their doses may be more affected by position shift. Therefore, there is a need to identify and adapt to such changes.

Abe et al. reported that the fiducial marker matching (MM) method could ensure coverage in carbon ion radiotherapy (CIRT) for primary hepatocellular carcinoma (HCC) [6]. Nevertheless, they found that the treatment planning dose distribution was reproducible for only one CT data set, indicating that the total delivered dose could not be derived from this result. Finding the true value of the total delivered dose could improve outcomes while minimizing damage to surrounding normal tissues.

Deformable image registration (DIR) applied to successive CT images can be used to determine the cumulative dose to mobile organs. Examples of this include Velec et al., who calculated the accumulated dose from daily cone beam CT (CBCT) [8], and Battista et al., who calculated the accumulated dose from daily megavoltage CT [9]. However, the success of intensity-based DIR largely depends on the image quality and contrast [10]. Additionally, particle therapy dose calculations are subject to large uncertainties, which are a characteristic of the beam range when image quality and contrast are low (such as in CBCT) [11,12]. To calculate accumulated doses with respect to intra- and inter-fractional variations, initial CT images need to be acquired using a high-resolution CT scanner at a time near to the commencement of

* Corresponding author at: Gunma University Heavy Ion Medical Center, 3-39-22 Showa-machi, Maebashi, Gunma 371-8511, Japan.
E-mail address: y_kubota@gunma-u.ac.jp (Y. Kubota).

https://doi.org/10.1016/j.radonc.2019.04.026
0167-8140/

treatment, and the effectiveness of MM should be re-evaluated on the accumulated dose.

The purpose of our study is to compare bone matching (BM) and fiducial MM methods on the accumulated dose in respect to intra- and inter-fractional changes in CIRT for HCC.

Materials and methods

Patients

This prospective study included ten consecutive patients with primary HCC who had been treated with four fractions of passive-irradiation CIRT at our facility between June 2017 and March 2018. The patients' characteristics are shown in Table 1. This study was approved by our facility's institutional review board and was registered at the University Hospital Medical Information Network Clinical Trials Registry (UMIN-CTR trial number: 000027125). All patients gave written informed consent, and their data were anonymized.

CT image acquisition

The study included four CT data sets, one acquired on each day of treatment, and one additional four-dimensional CT (4DCT), to investigate the effect of tumor movement and other intra- and inter-fractional changes on the cumulative dose. Gated end-expiration CT images for treatment planning (PlanCT) were acquired on a scanner (Aquilion LB®, Self-Propelled, Canon Medical Systems, Japan) in the simulation room. Also, the 4DCT images were reconstructed at the two time-points of the respiratory cycle during which radiation was "on" and the lungs were less than 30% maximum inflation, plus the time point of minimum inflation (defined as gate-in, gate-out, and expiration phases respectively). These images were used to measure the marker motion and calculate the PTV margins [13]. To mark the tumor position, gold markers were inserted near to the liver tumor before acquisition of the PlanCT in nine patients, while the lipiodol that had been used in previous tumor treatments was used for the other patient. The couch angle was adjusted within ± 15° around the longitudinal axis for each patient to avoid irradiating normal tissue as much as possible (as described in Table 1), and all CT images for each patient were acquired using the same patient-specific angle.

One CT data set was acquired on each of the four separate radiotherapy days. Additionally, a 5–10 min 4DCT was acquired in the treatment room on either the first or second radiotherapy day. The CT taken on that day was used as a reference CT (refCT) for dose accumulations. CT data sets were obtained with patients in the same position as that used for irradiation, and with the same tube voltage, tube current, field of view, and slice thickness settings used for the PlanCT and 4DCT, respectively.

Treatment planning

A radiation oncologist delineated gross tumor volume (GTV) on each PlanCT, and contoured a clinical target volume (CTV) by adding 5-mm margins to the GTV. Planning target volumes (PTV) were generated by anisotropically adding margins calculated by an established procedure [13]. Briefly, marker motions in each direction within the gating window were measured on the gate-in, gate-out, and expiration phase 4DCT images. Gate levels were reset if the dose distribution at the set margins was unacceptable. The patient-specific internal margins were calculated by adding one-third of the marker motion in each direction. The total margins were calculated from the square roots of the sum of the squares of the internal margins plus 3-mm of setup margin.

A treatment planning system (TPS) with a pencil-beam algorithm (XiO-N®, Elekta Sweden; Mitsubishi Electric, Japan) was used. The relative biological effectiveness (RBE) was included in the absorbed dose, and the clinical dose incorporating this was defined as Gy (RBE) [14].

At our facility, the prescribed dose for HCC is 60 Gy (RBE) delivered in four fractions using two beam directions (vertical and horizontal), and treatment plans that cover PTV V_{95} greater than 95%.

Calculating accumulated dose

To calculate the inter-fractional change (InterDoses), CT images acquired on three treatment days were registered to the refCT images using DIR, and warped dose distributions were then generated for the three CT image sets using the respective deformation matrices. The three warped dose distributions and the dose distribution for the refCT images were accumulated. The calculations were performed using commercial DIR software (MIM Maestro®, MIM Software, USA). Although intra-fractional changes can include random changes (e.g. bowel gas movement and other tissue movement) occurring over a few minutes to tens of minutes in a one-day treatment, only the accumulated dose distribution during the gating in the 4DCT was defined as the IntraDose in this study. To calculate the IntraDose, the CT images of the three 4DCT phases were registered to the refCT images with DIR, and the warped dose distributions of the three 4DCT phases were then generated using the respective deformation matrices. The following equation was used to correct the difference in the staying time for each phase:

$$Intra\ Dose = \frac{D_{GI}(t_{ExP} - t_{GI}) + D_{ExP}(t_{GO} - t_{GI}) + D_{GO}(t_{GO} - t_{ExP})}{2(t_{GO} - t_{GI})} \quad (1)$$

where D_{GI}, D_{GO}, and D_{ExP} are warped doses from the CT images of the gate-in, gate-out, and expiration phases, and t_{GI}, t_{GO}, and t_{ExP} are times acquired at the same three points. The InterDoses and IntraDoses were calculated with both BM and MM methods.

Table 1
Patient characteristics.

Patient	Sex	Age	Patient position	Roll angle (degree)	Irradiation direction	Tumor position	Marker object	Tumor volume (ml)
1	M	68	SP	345	AP, RL	S5	Metal	7.9
2	M	73	SP	345	AP, RL	S4	Metal	17.0
3	M	74	SP	5	AP, RL	S4	Metal	88.3
4	M	79	SP	15	AP, RL	S6	Metal	27.4
5	M	59	PR	0	PA, RL	S7	Metal	66.4
6	F	67	PR	0	PA, RL	S7	Metal	47.2
7	M	82	SP	15	AP, RL	S6	Lipiodol	23.4
8	M	80	PR	0	PA, RL	S6,7	Metal	104.3
9	F	81	SP	15	AP, RL	S8	Metal	14.0
10	M	71	PR	0	PA, RL	S7	Metal	37.1
Median		73.5		10				32.3

AP, anteroposterior; F, female; M, male; PR, prone position; PTV, planning target volume; RL, right–left; SP, supine position.

Data analysis

The tumor displacements for intra- and inter-fractional changes were measured from the BM and MM positions on all CT ($n = 40$) and 4DCT ($n = 30$) images using the software, and the displacement percentages were found to be within the total calculated margins. The registration used only translation in three directions (right–left [RL], anterior–posterior [AP], and superior–inferior [SI]; defined as + and − values respectively), because the CT images cannot be rotated for dose calculation in the XiO-N. The WELs of the vertical and horizontal beams were measured from the patient's body surface to the isocenters of each beam's direction plane. These measurements were performed using the TPS, with the BM and TM positions on the CT and 4DCT images. To evaluate the CTV on each CT data set, contours of the CTV on the PlanCT images were transferred to the CT images using rigid image registration (RIR) translation to the TM position.

The CTV V_{95}, the minimum doses covering more than 98%, 95%, and 90% of the CTV (D_{98}, D_{95}, D_{90}), and the conformity index (CI) [15] are shown in Eq. 2. The homogeneity index (HI) and the normal liver (volume of liver-CTV) receiving greater than 20 Gy (RBE; V_{20}) were used to evaluate the dose volume parameters of all 10 PlanDoses, 20 IntraDoses, and 20 Interdoses, for both BM and MM.

$$CI = \frac{CTV_{RI}^2}{CTV \times V_{RI}} \quad (2)$$

where V_{RI} = the volume receiving greater than 95% of the prescribed dose, andCTV_{RI} = the CTV receiving greater than 95% of the prescribed dose. Normal livers were recontoured onto each CT image.

To evaluate the optimal margins, CTVs that were isotropically enlarged or reduced from the PTV were defined as iCTVs. As the total margins were set to 3 mm in the treatment planning, when the measured marker motion was 0 within the gated 4DCT images, a contour that was 3 mm less than the PTV was defined as an iCTV with 0-mm margins. From these iCTVs, iCTVs were generated by adding margins of −3 to 5 mm; the V_{95} of each iCTV for the PlanDoses and InterDoses with BM and MM were evaluated. Margins with acceptance percentages of 95% (iCTV V_{95} greater than 95%) were calculated by fitting a sigmoid function.

Tumor movements and WEL changes were compared using *F*-tests. Normal distributions were compared using *t*-tests, and non-normal distributions were compared using Wilcoxon's test, after testing for normality with the Shapiro–Wilk test. A level of $p = 0.05$ was considered statistically significant. All statistical analyses were performed using SPSS software (IBM SPSS Statistics® for Windows, version 25.0, IBM, Inc., Armonk, NY, USA).

Results

The percentages of tumor movements were within their total margins (inter-fractional change: BM, 88.3%; MM, 93.3%; intra-fractional change: BM, 85.6%; MM, 91.1%). Tumor movements differed significantly between BM and MM methods in the SI and AP directions ($p < 0.001$ and $p = 0.002$, respectively). The percentages of changes in WEL were within their total margins (inter-fractional change: BM, 82.5%; MM, 90.0%; intra-fractional change: BM, 83.3%; MM, 88.3%) and are shown in Table 2. Sample images for each dose distribution with BM and MM are shown in Fig. 1. The InterDose and IntraDose dose–volume parameters are shown in Table 3. All cases were acceptable with either BM or MM, although all InterDose and IntraDose dose–volume histogram (DVH) parameters were better with MM than with BM.

The coverages and acceptance percentages for the iCTV margins are shown in Fig. 2. When the acceptance percentage was 95% according to the exponential function, these margins were −0.77 mm for the PlanDose, 4.19 mm for the InterDose with BM, and 0.76 mm for the InterDose with MM. The margins were smaller with MM than with BM.

Discussion

Although inter-fraction tumor movements and WEL changes with BM were greater than the total margins in 11.7% and 17.5% of cases respectively (Table 2), the InterDose and IntraDose CTV V_{95} values were acceptable in all cases. This may have been caused by a large CTV, which in turn may have caused the displacement error to be relatively small. Therefore, the decrease in coverage was small, but the non-irradiated volume increased. Doi et al. showed good local control for tumors less than 30 mm [16], suggesting that tumor volume and local control may be correlated. Therefore, it is unclear whether the relative CTV V_{95} is a good index for determining the dose distribution. Small tumor movements may have also caused the CTV V_{95} to be lower than the acceptance threshold. Abe et al. reported marker movements in the SI direction ranging from − 11.5 to 12.2 mm [6], while Case et al. and Lu et al. reported that tumor movements were greater than 10 mm in some cases [17,18]. The SI marker movements in this study were smaller than those reported previously (e.g., −7.75 to 8.28 mm for inter-fractional change).

CIRT radiation doses change greatly if the upstream object shifts along the beam path. Thus, heterogeneous tissues, such as lung and body/ribs in lung cancer [4,5,19], or bowel containing gas in pancreatic cancer, increase the risk of a decreased target dose [7]. In contrast, because HCC is relatively homogeneous, the WEL to the target changes very little (Table 2). Although the greatest change in WEL is thought to occur when the ribs are on the isocenter, these changes were small in this study (BM: vertical, 0.05 ± 3.06 mm; horizontal, 0.53 ± 2.39 mm; MM: vertical, 1.40 ± 2.60 mm; horizontal, −0.02 ± 1.81 mm), and may not have affected the CTV coverage. WEL varies more with BM than with MM, although its reproducibility with BM seems better than with MM, because bone affects it strongly. Thus, the coverage with MM seems to be better than that with BM.

The InterDose and IntraDose were acceptable in all cases (Table 3); however, all the CTV DVH parameters were better with MM than with BM, while the V_{20} of normal liver did not differ significantly between BM and MM. In some cases, the 95% isodose line of the InterDose was partially missing from the CTV with BM, although it was not missing with MM (Fig. 1). In clinical practice, both the intra- and inter-fractional effects would be included, even though they were considered separately in this analysis. If both the inter- and intra-fractional changes were included in the accumulated dose, the target coverage might decrease a little more than indicated by the inter-fractional change coverage alone, even though the IntraDose did not decrease as much as the InterDose (Table 3). It is evident from the results of our study that MM can ensure acceptable target coverage with smaller margins than BM (Fig. 2); therefore, we recommend MM over BM for CIRT of HCC.

The measured marker displacement was never greater than 10 mm. Clinically, marker displacement is measured using orthogonal X-ray images [20]. BM is used if the absolute marker movement is less than 3 mm, with MM if the absolute movement is 3–10 mm, and with a re-setup if the absolute movement is greater than 10 mm. Thus, we consider our treatment planning and patient positioning method to be reasonable because the outcomes of our treatment were good [21–23]. If any of the patients in this study were to suffer from local recurrence, we would not ascribe this to underdosing but to another cause, such as the difference in Gy [RBE] due to radiation resistance or hypoxic effects.

Our study has some limitations. We evaluated only ten patients, none of whom showed tumor displacement greater than 10 mm or

Table 2
Tumor motion and WEL change.

		Displacement [mm]						Ratio (less than margin) [%]		Ratio (less than 3 mm) [%]	
		BM			MM			BM	MM	BM	MM
		Mean	SD	Range	Mean	SD	Range				
Interfractional marker motion	RL	−0.02	1.44	−2.47–4.71							
	AP	0.43	1.76	−3.89–4.86							
	SI	0.04	3.38	−7.75–8.28							
	All	0.15	2.36	−7.75–8.28							
Interfractional tumor motion	RL	−0.39	2.37	−9.70–4.12	−0.35	1.89	−7.60–3.07	90.0	90.0	90.0	90.0
	AP	1.01	1.74	−2.29–4.73	0.81	1.22*	−1.24–3.62	85.0	90.0	85.0	90.0
	SI	0.66	3.27	−8.04–7.39	0.38	1.72*	−5.02–3.13	90.0	100	67.5	90.0
	All	0.43	2.62	−9.70–7.39	0.28	1.70*	−7.60–3.62	88.3	93.3	80.8	90.0
Intrafractional tumor motion	RL	0.32	2.22	−5.45–3.01	−0.27	1.64	−5.14–2.31	86.7	90.0	86.7	90.0
	AP	0.35	2.05	−3.52–5.43	0.22	1.70	−4.15–4.38	83.3	90.0	83.3	90.0
	SI	−1.00	3.26	−6.94–5.83	−1.58	2.62	−7.99–2.95	86.7	93.3	53.3	73.3
	All	−0.11	2.66	−6.94–5.83	−0.54	2.18	−7.99–4.38	85.6	91.1	80.8	84.4
Interfractional WEL change	V	0.05	3.03	−5.8–7.8	1.40	2.60	3.4–9.1	77.5	87.5	75.0	82.5
	H	−0.53	2.36	−9.8–3.5	−0.02	1.79	−3.1–3.3	87.5	92.5	87.5	90.0
	All	−0.24	2.73	−9.8–7.8	0.69	2.34	−3.1–9.1	82.5	90.0	83.3	86.3
Intrafractional WEL change	V	−0.96	3.06	−4.8–8.9	−0.25	2.50	−4.7–5.8	80.0	83.3	70.0	76.7
	H	−1.40	2.26	−9.2–−4.6	−0.57	1.71	−4.4–3.3	86.7	93.3	86.7	93.3
	All	−1.18	2.7	−9.2–−8.9	−0.41	2.15	−4.7–5.8	83.3	88.3	78.3	85.0

BM, bony structural matching; H, horizontal beam direction; MM, marker structural matching; V, vertical beam direction; WEL, water equivalent path length.
* $p < 0.05$ compared with BM.

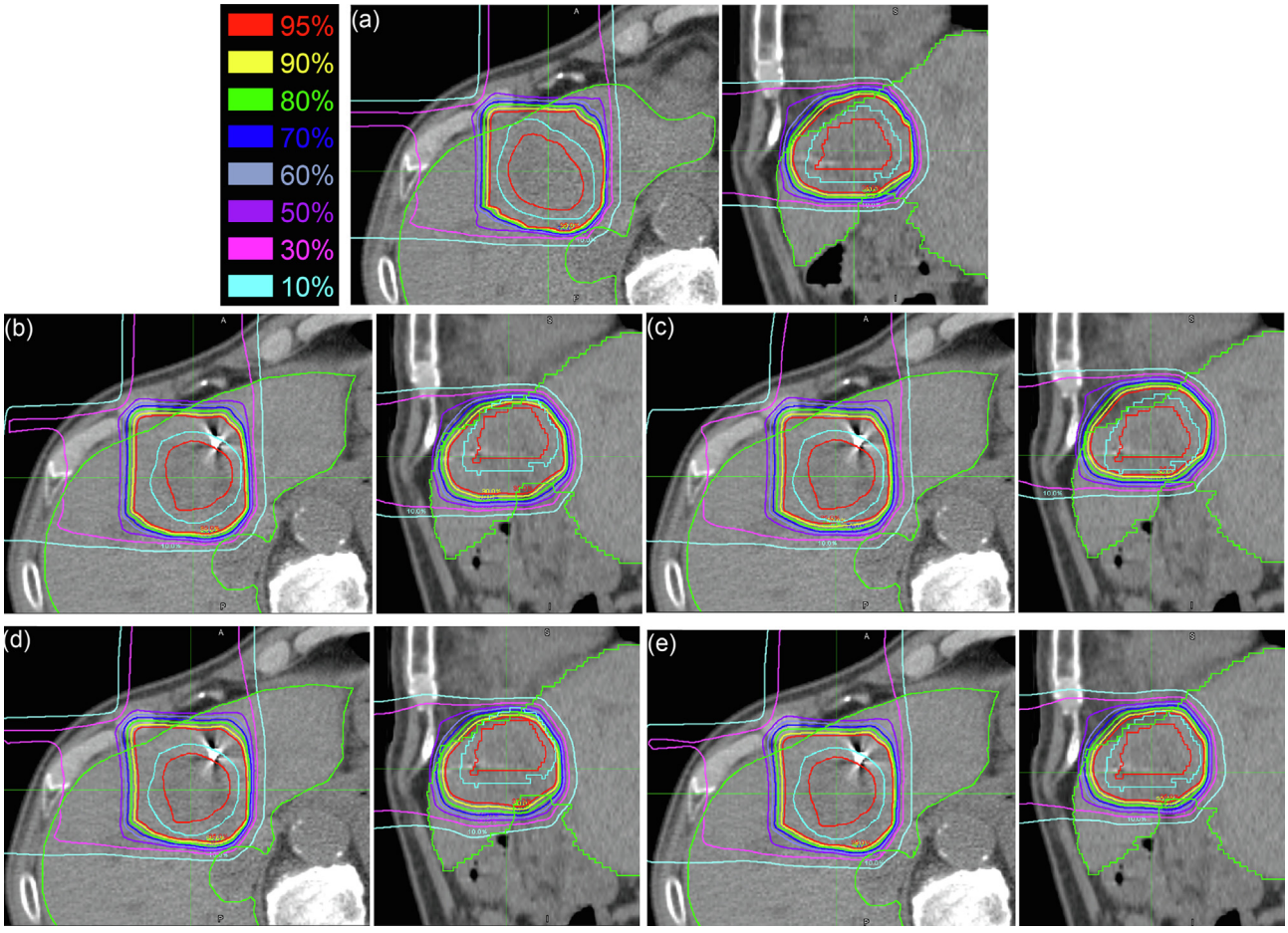

Fig. 1. Dose distributions. (a) PlanDose, (b, c) IntraDose, (e, f) InterDose, (b, d), bone matching (BM), (c, e) marker matching (MM). Left: axial plane; right: sagittal plane; red line: GTV, cyan lines: CTV; green lines: liver.

had target coverage greatly below the tolerance, indicating the need for further verification. The IntraDose was calculated using only the 4DCT images. To calculate the IntraDose more accurately, we would need to monitor patient motion and other parameters during irradiation. It is possible that some errors may have occurred in transferring the CTVs with RIR and the dose distribu-

Table 3
Dose–volume parameters.

Object	Parameter	PlanDose	IntraDose		InterDose	
			BM	MM	BM	MM
CTV	V_{95} (%)	99.94 (99.44–100)	99.46 (98.10–100)*	99.74 (98.91–100)*	98.74 (95.62–100)*	99.79 (98.55–100)
	D_{98} (Gy [RBE])	59.91 (59.48–60.14)	59.11 (57.10–60.15)*	59.52 (58.24–60.13)*	57.83 (51.63–60.20)*	59.54 (58.15–60.14)
	D_{95} (Gy [RBE])	60.04 (59.80–60.28)	59.80 (59.23–60.29)*	59.95 (59.44–60.28)*	59.31 (57.71–60.34)	59.96 (59.39–60.32)
	D_{90} (Gy [RBE])	60.13 (59.96–60.37)	60.07 (59.85–60.42)	60.10 (59.84–60.42)	60.01 (59.48–60.44)	60.11 (59.78–60.45)
	CI	0.49 (0.42–0.60)	0.51 (0.42–0.64)*	0.52 (0.43–0.62)*	0.52 (0.42–0.67)*	0.54 (0.44–0.66)*
	HI	1.03 (1.02–1.04)	1.03 (1.02–1.04)	1.03 (1.02–1.04)	1.03 (1.02–1.04)	1.03 (1.02–1.05)
Liver-CTV	V_{20} (ml)	151.56 (111.33–198.40)	150.10 (106.21–194.61)	150.34 (110.32–200.11)	148.01 (106.21–192.68)	151.99 (116.17–194.96)

Data are presented as mean (range). Note that BM and MM did not significantly differ.
BM, bony structural matching; CTV, clinical target volume; D_{90}, D_{95}, and D_{98}, minimum doses covering more than 90%, 95%, or 98% of the CTV; MM, marker structural matching; V_{20}, absolute volume of normal liver receiving greater than 20 Gy (RBE) (where Gy [RBE] is the clinical dose incorporating the relative biological efficiency included in the absorbed dose), V_{95}, percentage of CTV receiving greater than 95%.
* $p < 0.05$ compared with the planned dose.

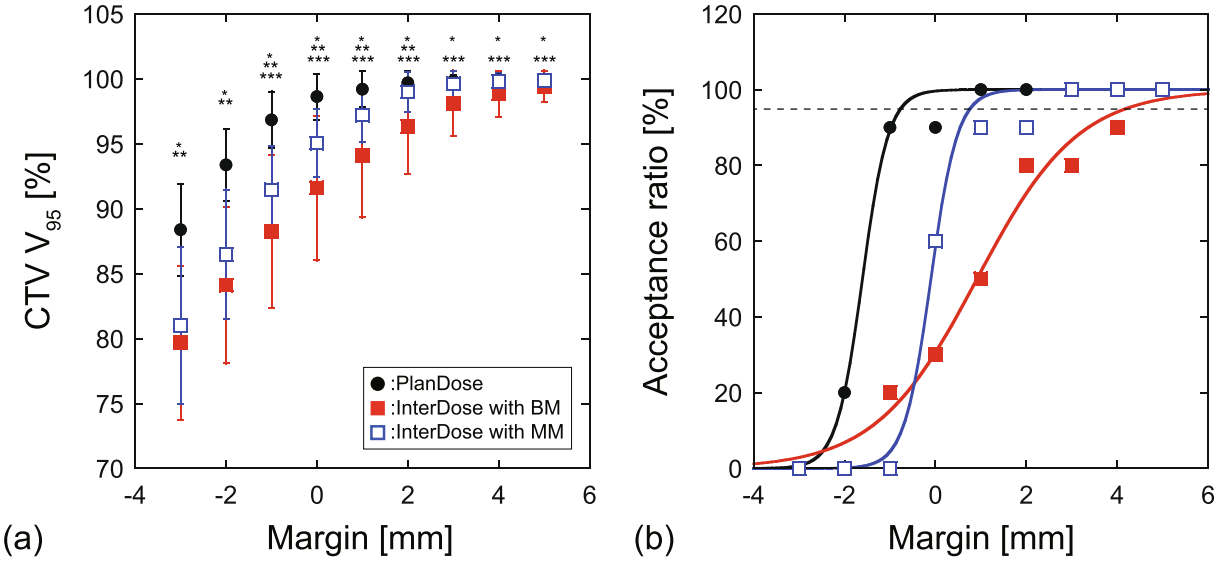

Fig. 2. Coverage and acceptance percentages for iCTV margins. (a) iCTV V_{95} (error bars: standard deviation). (b) Acceptance percentages with sigmoidal functions fitted (dashed line: 95% acceptance percentage). Black circles: PlanDose; red squares: InterDose with BM; blue squares: InterDose with MM. *$p < 0.05$ for PlanDose vs. InterDose with BM. **$p < 0.05$ for PlanDose vs. InterDose with MM. ***$p < 0.05$ for BM vs MM.

tions with DIR, and any such errors were not included in the analysis. These errors would appear as misdelineation of normal tissue as part of the CTV, and accumulating doses on the different points. Additionally, the evaluated tumors were never close to the bowel, and further dose limits are required for such cases, which may decrease the InterDose target coverage.

In this study, we prospectively evaluated the reproducibility of tumor movement and the accumulated doses for intra- and inter-fractional anatomical changes in CIRT for HCC. Our results indicate that the accumulated doses for inter- or intra-fractional changes were acceptable with BM or TM, confirming the high quality of our treatment planning and patient positioning methods. Additionally, we reconfirmed that MM is a better positioning technique than BM, demonstrating that it could ensure the target dose during and between fractions, and do this with smaller optimal margins. The positioning technique can be applied to multiple CIRT sites.

Conflicts of interest

None.

Funding

This research received no specific grant from any public, commercial, or not-for-profit funding agency.

Acknowledgements

The authors thank the radiology technologists, medical doctors, nurses, and medical physicists at GHMC for their valuable insights. The authors also thank Taku Miyabe at the Accelerator Engineering Corporation, Chiba, Japan, for technical support, and Drs. Damiana Chiavolini and Arnold Pompos at University of Texas Southwestern Medical Center, Dallas, Texas for editing a draft of this manuscript.

References

[1] Kraft G. Tumor therapy with heavy charged particles. Prog Part Nucl Phys 2000;45:S473–544.
[2] Bassler N, Kantemiris I, Karaiskos P, Engelke J, Holzscheiter MH, Petersen JB. Comparison of optimized single and multifield irradiation plans of antiproton, proton and carbon ion beams. Radiother Oncol 2010;95:87–93.
[3] Ohno T. Particle radiotherapy with carbon ion beams. EPMA J 2013;4:1–7.
[4] Irie D, Saitoh JI, Shirai K, et al. Verification of dose distribution in carbon ion radiation therapy for stage I lung cancer. Int J Radiat Oncol Biol Phys 2016;96:1117–23.
[5] Sakai M, Kubota Y, Saitoh JI, et al. Robustness of patient positioning for interfractional error in carbon ion radiotherapy for stage I lung cancer: Bone matching versus tumor matching. Radiother Oncol 2018;129:95–100.
[6] Abe S, Kubota Y, Shibuya K, et al. Fiducial marker matching versus vertebral body matching. Dosimetric impact of patient positioning in carbon ion radiotherapy for primary hepatic cancer. Phys Med 2017;33:114–20.
[7] Houweling AC, Fukata K, Kubota Y, et al. The impact of interfractional anatomical changes on the accumulated dose in carbon ion therapy of pancreatic cancer patients. Radiother Oncol 2016;119:319–25.

[8] Velec M, Moseley JL, Craig T, Dawson LA, Brock KK. Accumulated dose in liver stereotactic body radiotherapy: positioning, breathing, and deformation effects. Int J Radiat Oncol Biol Phys 2012;83:1132–40.
[9] Battista JJ, Johnson C, Turnbull D, Kempe J, Bzdusek K, Van Dyk J, et al. Dosimetric and radiobiological consequences of computed tomography-guided adaptive strategies for intensity modulated radiation therapy of the prostate. Int J Radiat Oncol Biol Phys 2013;87:874–80.
[10] Janssens G, de Xivry JO, Fekkes S, Dekker A, Macq B, Lambin P, et al. Evaluation of nonrigid registration models for interfraction dose accumulation in radiotherapy. Med Phys 2009;36:4268–76.
[11] Park YK, Sharp GC, Phillips J, Winey BA. Proton dose calculation on scatter-corrected CBCT image: Feasibility study for adaptive proton therapy. Med Phys 2015;42(8):4449–59.
[12] Arai K, Kadoya N, Kato T, Endo H, Komori S, Abe Y, et al. Feasibility of CBCT-based proton dose calculation using a histogram-matching algorithm in proton beam therapy. Phys Med 2017;33:68–76.
[13] Tashiro T, Ishii T, Koya J, et al. Technical approach to individualized respiratory-gated carbon-ion therapy for mobile organs. Radiol Phys Technol 2013;6:356–66.
[14] Kanai T, Endo M, Minohara S, et al. Biophysical characteristics of HIMAC clinical irradiation system for heavy-ion radiation therapy. Int J Radiat Oncol Biol Phys 1999;44:201–10.
[15] van't Riet A, Mak AC, Moerland MA, et al. A conformation number to quantify the degree of conformality in brachytherapy and external beam irradiation: Application to the prostate. Int J Radiat Oncol Biol Phys 1997;37:731–6.
[16] Doi H, Uemoto K, Suzuki O, Yamada K, Masai N, Tatsumi D, et al. Effect of primary tumor location and tumor size on the response to radiotherapy for liver metastases from colorectal cancer. Oncol Lett 2017;14:453-460.
[17] Case RB, Sonke JJ, Moseley DJ, Kim J, Brock KK, Dawson LA. Inter- and intrafraction variability in liver position in non-breath-hold stereotactic body radiotherapy. Int J Radiat Oncol Biol Phys 2009;75:302–8.
[18] Lu L, Diaconu C, Djemil T, Videtic GM, Abdel-Wahab M, Yu N, et al. Intra- and inter-fractional liver and lung tumor motions treated with SBRT under active breathing control. J Appl Clin Med Phys 2018;19:39–45.
[19] Kubota Y, Sakai M, Tashiro M, et al. Technical Note: Predicting dose distribution with replacing stopping power ratio for inter-fractional motion and intra-fractional motion during carbon ion radiotherapy with passive irradiation method for stage I lung cancer. Med Phys 2018;19:144–53.
[20] Kubota Y, Tashiro M, Shinohara A, et al. Development of an automatic evaluation method for patient positioning error. J Appl Clin Med Phys 2015;16:100–11.
[21] Shiba S, Abe T, Shibuya K, Katoh H, Koyama Y, Shimada H, et al. Carbon ion radiotherapy for 80 years or older patients with hepatocellular carcinoma. BMC Cancer 2017;17:721.
[22] Shiba S, Shibuya K, Katoh H, Koyama Y, Okamoto M, Abe T, et al. No deterioration in clinical outcomes of carbon ion radiotherapy for sarcopenia patients with hepatocellular carcinoma. Anticancer Res 2018;38:3579–86.
[23] Shibuya K, Ohno T, Katoh H, Okamoto M, Shiba S, Koyama Y, et al. A feasibility study of high-dose hypofractionated carbon ion radiation therapy using four fractions for localized hepatocellular carcinoma measuring 3 cm or larger. Radiother Oncol 2018. S0167-8140:33521-7. [Epub ahead of print].